

# Magnetic and thermodynamic properties of $\text{Li}_2\text{VO}_2\text{SiO}_4$ : a two-dimensional $S = 1/2$ frustrated antiferromagnet on a square lattice

R. Melzi, S. Aldrovandi, F. Tedoldi and P. Carretta\*

*Dipartimento di Fisica “A. Volta” e Unità INFN di Pavia, Via Bassi 6, 27100 Pavia, Italy*

P. Millet

*Centre d’Elaboration des Matériaux et d’Etudes Structurales, CNRS, 31055 Toulouse Cedex, France*

F. Mila

*Institut de Physique Théorique, Université de Lausanne, CH-1015 Lausanne, Switzerland*

(October 25, 2018)

## Abstract

NMR,  $\mu\text{SR}$ , magnetization and specific heat measurements in  $\text{Li}_2\text{VO}_2\text{SiO}_4$  powders and single crystals are reported. Specific heat and magnetization measurements evidence that  $\text{Li}_2\text{VO}_2\text{SiO}_4$  is a frustrated two-dimensional  $S = 1/2$  Heisenberg antiferromagnet on a square lattice with a superexchange coupling  $J_1$ , along the sides of the square, almost equal to  $J_2$ , the one along the diagonal ( $J_2/J_1 = 1.1 \pm 0.1$  with  $J_2 + J_1 = 8.2 \pm 1$  K). At  $T_c \simeq 2.8$  K a phase transition to a low temperature collinear order is observed.  $T_c$  and the sublattice magnetization, derived from NMR and  $\mu\text{SR}$ , were found

---

\*e-mail: carretta@fisicavolta.unipv.it

practically independent on the magnetic field intensity up to 9 Tesla. The critical exponent of the sublattice magnetization was estimated  $\beta \simeq 0.235$ , nearly coincident with the one predicted for a two-dimensional XY system on a finite size. The different magnetic properties found above and below  $T_c$  are associated with the modifications in the spin hamiltonian arising from a structural distortion occurring just above  $T_c$ .

PACS numbers: 76.60.Es, 75.40.Gb, 75.10.Jm

## I. INTRODUCTION

In recent years one has witnessed an extensive investigation of quantum phase transition in low-dimensional  $S = 1/2$  Heisenberg antiferromagnets (QHAF) as a function of doping, magnetic field and disorder<sup>1</sup>. For example, two-dimensional QHAF (2DQHAF) have been widely studied in order to evidence a phase transition from the renormalized classical to the quantum disordered regime upon charge doping<sup>2</sup>. Another possibility to drive quantum phase transitions in a 2DQHAF is to induce a sizeable frustration. In particular, for a square lattice with an exchange coupling along the diagonal  $J_2$  about half of the one along the sides of the square  $J_1$  (see Fig. 1a), a crossover to a spin-liquid ground state is expected<sup>3–5</sup>. For  $J_2/J_1 \lesssim 0.35$  Néel order is realized, while for  $J_2/J_1 \gtrsim 0.65$  a collinear order should develop. The collinear order (see Fig. 1a), which can be considered as formed by two interpenetrating Néel sublattices with staggered magnetization  $\mathbf{n}_1$  and  $\mathbf{n}_2$ , is characterized by an Ising order parameter  $\sigma = \mathbf{n}_1 \cdot \mathbf{n}_2 = \pm 1$ <sup>6</sup>. The two values of  $\sigma$  correspond to the two collinear configurations which can develop at low temperature (hereafter  $T$ ), one with spins ferromagnetically aligned along the  $x$  axis, corresponding to a magnetic wave-vector  $\mathbf{Q} = (0, \pi/a)$ , the other with spins ferromagnetically aligned along the  $y$  axis ( $\mathbf{Q} = (\pi/a, 0)$ ). At a certain temperature  $T_c$  a phase transition occurs and the system chooses among the  $x$  or  $y$  collinear configurations. The precise boundaries of the  $J_2/J_1$  phase diagram for a frustrated 2DQHAF are unknown and could be modified by the presence of a finite third neighbour coupling<sup>6</sup>. Most of these theoretical predictions have not found an experimental support so far, mainly due to the absence of systems which can be regarded as prototypes of frustrated 2DQHAF on a square lattice with  $J_2$  close to  $J_1$ , even if some frustrated 2DQHAF with different topologies have been recently studied<sup>7</sup>. Moreover, a theoretical description of the spin dynamics of these frustrated 2DQHAF as a function of  $T$  and magnetic field intensity is still missing.

Recently, two vanadates which can be considered as prototypes of frustrated 2DQHAF on a square lattice have been discovered<sup>8</sup>:  $\text{Li}_2\text{VO}\text{SiO}_4$  and  $\text{Li}_2\text{VO}\text{GeO}_4$ . These two isostructural

compounds are characterized by a layered structure containing  $V^{4+}$  ( $S = 1/2$ ) ions<sup>9</sup> (see Fig. 1b). The structure of  $V^{4+}$  layers suggests that the superexchange couplings between first and second neighbours are similar. It is however difficult a priori to decide which one should dominate: first neighbours are connected by two superexchange channels, but they are located in pyramids looking in opposite directions and are not exactly in the same plane, whereas second neighbours are connected by one channel, but are located in pyramids looking in the same directions and are in the same plane. On the basis of NMR and susceptibility it has been possible to demonstrate that in  $\text{Li}_2\text{VOSiO}_4$   $J_2/J_1$  is of the order of unity and that the ground state is collinear<sup>8</sup>, as expected for  $J_2/J_1 \gtrsim 0.65$ <sup>6</sup>.

In this paper we present a detailed study of the magnetic and thermodynamic properties of  $\text{Li}_2\text{VOSiO}_4$  by means of NMR,  $\mu\text{SR}$ , magnetization and specific heat measurements. In particular, we show that the spin dynamic and static properties above the collinear ordering temperature  $T_c$  are consistent with the ones theoretically predicted for a frustrated 2DQHAF with  $J_2/J_1 \simeq 1$ . The phase transition to the collinear phase seems to be triggered by a structural distortion occuring just above  $T_c$ , which possibly modifies the superexchange couplings and lifts the degeneracy among the two ground state configurations. The critical exponent of the sublattice magnetization and the independence of  $T_c$  on the magnetic field intensity up to 9 Tesla, suggest that the transition is driven by the XY anisotropy.

The paper is organized as follows: in Section II we present the experimental results obtained by each technique; in Section III we discuss the experimental results in the light of numerical and analytical results for frustrated 2DQHAF on a square lattice, first for  $T > T_c$  and then for  $T < T_c$ ; the main conclusions are summarized in Section IV.

## II. EXPERIMENTAL ASPECTS AND EXPERIMENTAL RESULTS

### A. Sample Preparation, Specific Heat and Magnetization

$\text{Li}_2\text{VOSiO}_4$  was prepared by solid state reaction starting from a stoichiometric mixture of  $\text{Li}_2\text{SiO}_3$ ,  $\text{V}_2\text{O}_3$  and  $\text{V}_2\text{O}_5$  according to the procedure described in Ref. 9. The sample was analyzed by X-ray powder diffraction (XRD) using a Seifert C3000 diffractometer with  $\text{CuK}\alpha$  radiation and then pressed into a 1 g pellet followed by a short sintering in vacuum at 800 C for 6 hours. Single crystals, of average size  $1 \times 1 \times 0.2 \text{ mm}^3$ , were obtained from  $\text{Li}_2\text{VOSiO}_4$  powder heated at 1150 C for 2 hours, slowly cooled at a rate of 5 C/hour down to 1000 C and then furnace cooled down to room temperature.

Specific heat ( $C(T)$ ) measurements have been performed on a sintered pellet of  $\text{Li}_2\text{VOSiO}_4$  by using a standard homemade adiabatic calorimeter. The contribution of the addenda decreased from about 5% to below 1% of the total heat capacity on decreasing  $T$  from 25 K to 2.5 K. At low  $T$  the specific heat shows a broad maximum due to the correlated spin excitations and a sharp peak around 2.8 K (see Fig. 2a) associated with a second order phase transition, as can be inferred from the non-singular behaviour of the entropy around 2.8 K. Above 20 K a rapid increase, originating from phonon excitations is observed (see Fig. 2a). In order to accurately estimate the magnetic contribution  $C^m(T)$  (Fig. 2b) to the specific heat one has to subtract the phonon term  $C^p(T)$ , extrapolated to low  $T$ .  $C^p(T)$  was observed to follow a Debye law from 20 to 70 K, namely

$$C^p(T) = 9Nk_B \left(\frac{T}{\Theta_D}\right)^3 \int_0^{\frac{\Theta_D}{T}} \frac{x^4 e^x}{(e^x - 1)^2} dx, \quad (1)$$

with  $\Theta_D \simeq 280 \text{ K}$  the Debye temperature. It must be stressed that below 15 K  $C^p(T)$  is negligible with respect to  $C^m(T)$ , therefore, any incorrect extrapolation of  $C^p(T)$  to low  $T$  will not affect the estimate of  $C^m(T)$  below 15 K.

Magnetization measurements were carried out with a Quantum Design MPMS-XL7 SQUID magnetometer, both on powders and on single crystals. The  $T$  dependence of the spin susceptibility  $\chi = M/H$  is shown in Fig. 3. One observes a high  $T$  Curie-like behaviour, a low  $T$  maximum around 5 K and a kink at  $T_c \simeq 2.8 \text{ K}$ , the same temperature where a peak

in the specific heat is detected. The kink is better evidenced if one reports the derivative of the susceptibility  $d\chi/dT$  (see the upper inset to Fig. 3). The susceptibility above 15 K can be appropriately fitted by

$$\chi(T) = \chi_{VV} + c_\chi/(T + \Theta), \quad (2)$$

where  $\Theta$  is the Curie-Weiss temperature,  $c_\chi = N_A g^2 S(S+1) \mu_B^2 / 3k_B$  ( $g$  the Landé factor and  $\mu_B$  the Bohr magneton) is the Curie constant and  $\chi_{VV}$  the Van-Vleck term. The best fit of the data in the  $T$  range 10-300 K yields  $\Theta = 8.2 \pm 1$  K<sup>10</sup>,  $c_\chi = 0.34$  emu K/mole and  $\chi_{VV} = 4 \times 10^{-4}$  emu/mole. We point out that the value of  $c_\chi$  is in good quantitative agreement with what one would expect for an  $S = 1/2$  paramagnet, while the absolute value of  $\chi_{VV}$  is consistent with a separation between the  $d_{xy}$  ground state and the first excited  $t_{2g}$  levels of the order of 0.15 eV, which is typical for  $V^{4+}$  in a pyramidal environment<sup>11</sup>. Below  $T_c$  the  $T$  dependence of the susceptibility for magnetic fields  $H \parallel c$  and  $H \perp c$  is different, as expected in the presence of long range order. In particular, one observes that while for  $H \perp c$  the susceptibility progressively diminishes on decreasing temperature, for  $H \parallel c$  it flattens (see the lower inset to Fig. 3), suggesting that  $V^{4+}$  magnetic moments lie in the  $ab$  plane.

The magnetic field dependence of  $T_c$ , derived either from the kink in the susceptibility or from the maximum in  $d\chi/dT$ , was measured from 0.1 up to 7 Tesla, where the Zeeman energy  $g\mu_B H$  is greater than  $k_B \Theta$ , and, remarkably,  $T_c$  was not observed to vary by more than 0.07 K, i.e. less than  $0.03T_c$  (see Fig. 4).

## B. $\mu$ SR

Zero field (ZF)  $\mu$ SR measurements have been carried out on  $\text{Li}_2\text{VO SiO}_4$  powders at ISIS pulsed source, both on EMU and MUSR beamlines, using spin-polarized 29 MeV/c muons. The time evolution of the muon polarization is characterized by a constant background, due to the sample holder and cryostat walls, and by a fast decay which progressively changes from

exponential (see Fig. 5) to gaussian on increasing temperature, for  $T > T_c$ . Below  $T_c$  both oscillating and non-oscillating components are evident, the second one with an amplitude about half of the former one, as usually expected in magnetic powders with equivalent muon sites<sup>12</sup>. It must be mentioned that below  $T_c$  around 10% of the total asymmetry is missing, possibly due to fast precessing muons which cannot be detected at a pulsed muon source. Summarizing, below  $T_c$  the time evolution of the muon polarization was fitted according to

$$P_\mu(t) = A_{back} + A_1 e^{-\sigma t} \cos(\gamma B_\mu t + \phi) + A_2 e^{-\lambda t}, \quad (3)$$

where  $A_{back}$  is the sample holder background,  $A_1$  is the amplitude of the oscillating component, with  $\gamma = 2\pi \times 135.5$  MHz/Tesla the  $\mu^+$  gyromagnetic ratio and  $B_\mu$  the local field at the  $\mu^+$ , while  $A_2$  is the amplitude of the non-oscillating component with  $\lambda$  the longitudinal decay rate. Above  $T_c$  the polarization was fitted by

$$P_\mu(t) = A_{back} + A e^{-\lambda t} e^{-\sigma_N^2 t^2 / 2} \quad (4)$$

where the exponential term is the relaxation induced by the progressive slowing down of the  $V^{4+}$  spin fluctuations on decreasing temperature, while the gaussian term should originate from nuclear dipolar interaction. In particular, it is likely that  $\mu^+$  localizes close to the apical oxygens, where it is coupled to  $^7\text{Li}$  nuclear magnetic moments. The gaussian relaxation rate was estimated  $\sigma_N = 0.34 \pm 0.01 \mu\text{s}^{-1}$ , for  $T_c \leq T \leq 4.2$  K, a value typical for relaxation driven by nuclear dipole interaction<sup>12</sup>.

The  $T$  dependence of the local field at the muon  $B_\mu$  and of the longitudinal relaxation rate  $\lambda$ , derived after the fit of the data with Eqs. 3 and 4, are reported in Figs. 6 and 7, respectively.  $B_\mu(T)$ , which yields the  $T$  dependence of  $V^{4+}$  average magnetic moment, is characterized by a sharp but continuous decrease on approaching  $T_c$ , while  $\lambda(T)$  is characterized by a divergence at  $T_c$ , as expected for a second order phase transition.

### C. $^7\text{Li}$ and $^{29}\text{Si}$ NMR

$^7\text{Li}$  ( $I = 3/2$ ) NMR measurements have been carried out both on single crystals and powders, while  $^{29}\text{Si}$  ( $I = 1/2$ ) NMR, due to the reduced sensitivity could be performed only in powder samples. The measurements have been performed using standard NMR pulse sequences. In particular, the spectra have been recorded by Fourier transform of half of the echo signal when the line was completely irradiated or by summing spectra recorded at different frequencies when it was only partially irradiated. The NMR resonance frequency of  $^7\text{Li}$  was observed to shift to high frequencies on decreasing temperature, with a trend identical to the one of the macroscopic susceptibility (Fig.3). In fact, for  $^7\text{Li}$  NMR shift one can write

$$^7\Delta\mathcal{K}(T) = \frac{\sum_j \mathcal{A}_j \chi(T)}{g\mu_B N_A} + \delta \quad (5)$$

where  $\mathcal{A}_j$  is the hyperfine coupling tensor with the  $j$ -th  $\text{V}^{4+}$  and  $\delta$  the chemical shift. A  $T$  dependent shift was observed both in the single crystals and in the powders, evidencing a sizeable transferred hyperfine interaction of  $\text{V}^{4+}$  spins with  $^7\text{Li}$  nuclei. From the plot of the shift versus the susceptibility (Fig. 8) the hyperfine coupling constants and the chemical shift were determined. It turns out that  $\delta = -70 \pm 30$  ppm and that the hyperfine field at  $^7\text{Li}$  is given by

$$\vec{h} = \sum_j (\mathcal{A}_{dip})_j \vec{S}_j + \sum_{i=1,2} A_t \vec{S}_i \quad (6)$$

where  $\mathcal{A}_{dip}$  is the dipolar coupling with  $\text{V}^{4+}$  ions, while  $A_t = 850$  Gauss is the transferred coupling, which is supposed to arise from the two  $\text{V}^{4+}$  nearest neighbours only. On the other hand,  $^{29}\text{Si}$  NMR resonance frequency in the powders is constant from room temperature down to 4 K, pointing out that the hyperfine coupling is of purely dipolar origin in this case.

Below  $T_c$ , in the single crystals, for  $H \parallel c$ ,  $^7\text{Li}$  NMR spectrum splits in three lines (see Fig. 9): a central one with an intensity about twice of that of two equally spaced satellites. The two satellites correspond to  $^7\text{Li}$  sites with hyperfine fields of equal intensity but opposite



orientations, while the central line corresponds to  $^7\text{Li}$  sites where the hyperfine field cancels out<sup>8</sup>. The  $T$  dependence of the satellites shift is proportional to the amplitude of  $\text{V}^{4+}$  magnetic moment and, therefore, it is another method, besides ZF  $\mu\text{SR}$ , to determine the temperature dependence of the sublattice magnetization (see Fig. 10).

$^{29}\text{Si}$  NMR powder spectrum shows a quite different behaviour at low  $T$ . Around 3 K, still above  $T_c$ , one observes the appearance of a shifted narrow peak (see Fig. 11). On decreasing  $T$  the low-frequency peak progressively disappears, while the intensity of the high frequency one increases. This jump in  $^{29}\text{Si}$  NMR shift has to be associated either with a modification of the chemical shift or of the hyperfine coupling, suggesting the occurrence of a structural distortion just above  $T_c$ . It has to be noticed that, on the contrary, no anomaly was detected in  $^7\text{Li}$  spectra around 3 K. Below  $T_c$   $^{29}\text{Si}$  NMR linewidth is very close to the one above  $T_c$ , indicating that the local field at  $^{29}\text{Si}$  site is zero.

Nuclear spin-lattice relaxation rate  $1/T_1$  was measured by exciting the nuclear magnetization either with a comb of saturating pulses or with a  $180^\circ$  pulse (inversion recovery sequence). Both for  $^7\text{Li}$  and  $^{29}\text{Si}$  the recovery of nuclear magnetization towards equilibrium was a single exponential, indicating that for  $^7\text{Li}$  also the  $\pm 3/2 \rightarrow \pm 1/2$  lines were sizeably irradiated during the measurements. In fact, at room temperature one can discern the  $\pm 3/2 \rightarrow \pm 1/2$  lines shifted by  $\simeq 40$  kHz from the  $+1/2 \rightarrow -1/2$ <sup>13</sup>. The  $T$  dependence of  $^7\text{Li}$   $1/T_1$  is shown in Fig. 12. One observes that  $1/T_1$  is constant from room temperature down to  $\simeq 3.2$  K, then shows a peak at  $T_c$  and rapidly decreases in the ordered phase.  $^{29}\text{Si}$   $1/T_1$  shows a similar  $T$  dependence below 4.2 K (Fig. 13), its absolute value, however, is about two orders of magnitude smaller, supporting the conclusion in favour of a hyperfine coupling of purely dipolar origin.

### III. DISCUSSION

### A. Above $T_c$

The  $T$  dependence of the susceptibility and of the specific heat allows to derive information on the basic parameters of the electron spin hamiltonian, namely the coupling constants and their ratio  $J_2/J_1$ . For a non-frustrated  $S = 1/2$  2D Heisenberg AF on a square lattice the Curie-Weiss temperature  $\Theta = J_1$  nearly coincides with the temperature where the susceptibility displays a maximum and one has  $T_m^x = 0.935\Theta^{14}$ . On the other hand, in  $\text{Li}_2\text{VO}_2\text{SiO}_4$   $\Theta = J_2 + J_1 = 8.2 \pm 1$  K is significantly larger than  $T_m^x = 5.35$  K (see Fig. 3), as expected for a frustrated system. By comparing the measured ratio  $T_m^x/\Theta = 0.65 \pm 0.07$  with exact diagonalization and quantum Monte Carlo (QMC) results it is possible to estimate  $J_2/J_1^8$ . It turns out that  $J_2/J_1$  is close either to 0.25 or 2.5<sup>8</sup>, however, it is not possible to say which of the two coupling constants is larger. We remark that these two values were estimated by assuming  $\Theta = 8.2$  K, however, taking into account the uncertainty of  $\pm 1$  K in the estimate of Curie-Weiss temperature and that exact diagonalizations provide useful estimates for  $J_2/J_1 < 0.4$ , while QMC simulations only for  $J_2/J_1 \gtrsim 2^8$ , it is difficult to assign an error bar to these estimates of  $J_2/J_1$ .

A more accurate determination of the ratio  $J_2/J_1$  can be done by analyzing  $C^m(T)$  data in the light of diagonalization results by Singh and Narayanan<sup>15</sup> and of the numerical calculations by Bacci et al.<sup>16</sup>. From the numerical results reported in Refs. 15 and 16 it is possible to plot the amplitude of the specific heat at the maximum  $C^m(T_m^C)$  as a function of the ratio  $J_2/J_1$  (Fig. 14a). It turns out that the value  $C^m(T_m^C) = (0.436 \pm 0.004)R$  found for  $\text{Li}_2\text{VO}_2\text{SiO}_4$  ( $R = N_A k_B$ ) (see Fig. 2) is compatible only with  $J_2/J_1 = 0.44 \pm 0.01$  or  $1.1 \pm 0.1$  (Fig. 14a). To discriminate among the two ratios one can analyze how  $T_m^C = 3.5 \pm 0.1$  K varies as a function of  $J_2/J_1$ . Since

$$\frac{T_m^C}{J_1} = \frac{T_m^C}{\Theta} \left(1 + \frac{J_2}{J_1}\right), \quad (7)$$

with  $T_m^C/\Theta = 0.42 \pm 0.04$ , one can check which value of  $J_2/J_1$  is compatible with the results of  $T_m^C/J_1$  vs.  $J_2/J_1$  reported by Singh and Narayanan<sup>15</sup> (see Fig. 14b). One observes that

Eq. 7 is satisfied only for  $J_2/J_1$  around 0.1 or 1.1. Therefore, the only solution which is compatible with the experimental values both of  $T_m^C$  and  $C(T_m^C)$  is  $J_2/J_1 = 1.1 \pm 0.1$ . This also indicates that  $\Theta$  is close to 9 K (see Fig. 14b) and that  $T_m^X/\Theta \simeq 0.59$ . Now, by assuming this value for  $T_m^X/\Theta$  one would derive from the analysis of the susceptibility a value  $J_2/J_1 \lesssim 2$ , in agreement with the specific heat analysis, even if an accurate estimate with QMC is prevented, since in this range of  $J_2/J_1$  the results start to suffer from the minus sign problem. A value of  $J_2/J_1$  around 1.1 also implies that  $\text{Li}_2\text{VOSiO}_4$  lies on the right hand side of the phase diagram reported in Fig. 1a, where the ground state is expected to be a collinear phase, in complete agreement with NMR results below  $T_c$  (see later on).

Further information on the superexchange constants can be achieved from the analysis of  $^7\text{Li}$   $1/T_1$ . In the limit  $T \gg J_1 + J_2$ ,  $1/T_1$  is constant (see Fig. 12) and, by resorting to the usual gaussian form for the decay of the spin correlation function, one can write<sup>17</sup>

$$(1/T_1)_\infty = \frac{\gamma^2}{2} \frac{S(S+1)}{3} \frac{\sqrt{2\pi}}{\omega_E} \times \sum_{k,i,j} |A_{ij}^k|^2 \quad (8)$$

with  $A_{ij}^k$  ( $i, j = x, y, z$ ) the components of the hyperfine tensor due to the  $k^{\text{th}}$   $\text{V}^{4+}$  and  $\gamma$  the nuclear gyromagnetic ratio.  $\omega_E = \sqrt{J_1^2 + J_2^2} (k_B/\hbar) \sqrt{2zS(S+1)/3}$  is the Heisenberg exchange frequency, where  $z = 4$  is the number of nearest neighbour spins of a  $\text{V}^{4+}$  coupled either through  $J_1$  or  $J_2$ . By using in Eq. 8  $(1/T_1)_\infty = 0.2 \text{ ms}^{-1}$ , i.e.  $^7\text{Li}$  relaxation rate in the  $T$  range 300 – 3.2 K, one finds  $\sqrt{J_1^2 + J_2^2} \simeq 8.7 \text{ K}$ , close to what one would derive from susceptibility and specific heat measurements.

On decreasing temperature  $^7\text{Li}$  and  $^{29}\text{Si}$   $1/T_1$  remain constant down to 3.2 K, at variance with  $\mu^+$   $1/T_1$  (usually called  $\lambda$ ), which diverges on decreasing  $T$ , already at 4.2 K, due to the growth of the AF correlations. Both for nuclei and  $\mu^+$  the spin-lattice relaxation is induced by the fluctuations of the effective local field, driven by the correlated spin dynamics, and one can write

$$1/T_1 \equiv \lambda = \frac{\gamma^2}{2N} \sum_{\vec{q}, \alpha} |A_{\vec{q}}|^2 S_{\alpha\alpha}(\vec{q}, \omega_R) \quad (9)$$

where  $|A_{\vec{q}}|^2$  is the hyperfine form factor and  $S_{\alpha\alpha}(\vec{q}, \omega_R)$  ( $\alpha = x, y, z$ ) are the components of the dynamical structure factor at the NMR or  $\mu\text{SR}$  resonance frequency. One immediately

realizes that a different trend of NMR and  $\mu$ SR  $1/T_1$  can originate from the different form factors, which couple each one of these probes in a different way with the spin excitations at the critical wave-vector. In particular, one might suspect that  $^7\text{Li}$  and  $^{29}\text{Si}$  form factors filter out the AF correlated spin excitations. However, if one considers that  $^7\text{Li}$  is coupled via a transferred hyperfine interaction with  $\text{V}^{4+}$  nearest neighbours (see Eq. 6), one finds that  $^7\text{Li}$  form factor is little  $\vec{q}$ -dependent and that no filtering of the AF excitations can be envisaged. Moreover, the divergence of  $^7\text{Li}$  and  $^{29}\text{Si}$   $1/T_1$  at  $T_c$  evidences that the fluctuations at the critical wave vectors cannot be completely filtered out.

Another relevant difference is still present between  $\mu$ SR and NMR measurements. While the former were performed in zero field, NMR  $1/T_1$  measurements were carried out in magnetic fields ranging from 1.8 to 9 Tesla, at which the Zeeman energy is comparable to the superexchange couplings. Therefore, it is tempting to associate the different behaviour of NMR and  $\mu$ SR spin-lattice relaxation rates above  $T_c$  to a crossover of regime induced by the magnetic field. In particular, the  $T$  independent  $T_1$  measured in NMR would be consistent with a quantum critical regime<sup>18</sup>, while the exponential divergence of  $1/T_1$  ( $\lambda$ ) measured with  $\mu$ SR would be consistent with a renormalized classical regime<sup>18</sup>, where, by resorting to classical scaling arguments for 2D systems, one can write<sup>19</sup>

$$1/T_1(T) \equiv \lambda(T) \propto \xi(T) = 0.493a \times e^{2\pi\rho_s/T} \left[ 1 - 0.43 \frac{T}{J} + O\left(\frac{T}{J}\right)^2 \right] \quad (10)$$

with  $\xi$  the in-plane correlation length,  $a$  the lattice step and  $\rho_s$  the spin stiffness. From the  $T$  dependence of  $\lambda$  (see Fig. 7) above  $T_c$  one derives  $2\pi\rho_s = 7.4$  K, less than the value  $1.15\Theta$  expected for a non-frustrated system<sup>20</sup>.

## B. Below $T_c$

Since  $\text{V}^{4+}$  magnetic moments lie in the  $ab$  plane, as suggested by susceptibility measurements (Fig. 3) and by the EPR analysis of the  $g$  tensor<sup>21</sup>, and provided that the dipolar magnetic field cancels at  $^{29}\text{Si}$  site, one realizes that the order must be collinear with a critical wave vector  $\mathbf{Q} = (\pi/a, 0)$ , where  $x$  is the direction of the magnetic moments<sup>8</sup>.

The second order transition to the low  $T$  collinear phase is evidenced by the peaks in  $1/T_1$  and in  $d\chi/dT$ . It is remarkable to observe that  $T_c$  is practically field independent up to at least 9 Tesla (see Fig. 4), where  $g\mu_B H/k_B > J_1 + J_2$ , while a decrease is expected, with  $T_c$  vanishing for  $g\mu_B H \simeq 6k_B J_2$ , if  $J_2/J_1 \simeq 1$ , i.e. at  $H \simeq 20$  Tesla<sup>22</sup>. A possible explanation for this peculiar behaviour is that the structural distortion occuring just above  $T_c$ , deduced from  $^{29}\text{Si}$  NMR spectra, causes an increase in the coupling constants and that even at 9 Tesla  $g\mu_B H/k_B < J_1 + J_2$ . Another possibility is that  $\text{Li}_2\text{VOSiO}_4$  is a 2D XY system with  $T_c$  close to the corresponding Berezinskii-Kosterlitz-Thouless transition<sup>22</sup>.

Also the  $T$  dependence of the sublattice magnetization, derived either from the local field at the muon or from the splitting of  $^7\text{Li}$  NMR line, was found independent on the magnetic field intensity from zero up to 9 Tesla. From ZF $\mu$ SR measurements it has been possible to derive a critical exponent  $\beta = 0.235 \pm 0.009$  for the sublattice magnetization (see Fig. 6). Remarkably, this value of  $\beta$  is very close to the one predicted for a 2D XY model on a finite size<sup>23</sup>. Although some in-plane anisotropy can be discerned from the susceptibility data just above  $T_c$  (see the inset to Fig. 3), there is no evidence of a crossover from Heisenberg to XY in the  $T$  dependence of the correlation length, derived from  $\lambda(T)$  above  $T_c$ <sup>24</sup>. It is also interesting to observe that the sublattice magnetization measured by means of  $\mu$ SR shows a slight high  $T$  tail, as expected in a finite size system<sup>23</sup>. If the order is purely 2D, without long range order along the  $c$  axis, one would expect  $^7\text{Li}$  nuclei, which lie between  $\text{V}^{4+}$  layers, to be characterized by a broad powder-like NMR spectrum. This is certainly not the case for  $T_c - T \gtrsim 0.2$  K (see Fig. 9), however one cannot exclude from the NMR measurements that the order is 2D in the very vicinity of  $T_c$ . In fact, since the strong in-plane XY correlations enhance the 3D coupling the difference between the 2DXY and 3D ordering temperatures is expected to be small, of the order of the interlayer coupling  $J_\perp$ <sup>25</sup>. An upper limit for  $J_\perp$  can be estimated by assuming that  $T_c$  is the 3D ordering temperature of a Heisenberg AF, where  $T_c \simeq 0.4J_\perp \xi^2(T_c)$ <sup>26</sup>. From the temperature dependence of  $\mu^+$  relaxation rate  $\lambda$  (see Eq. 10) one finds  $\xi(T_c)/a \simeq 5.3$ , leading to  $J_\perp \simeq 0.2$  K. This value is possibly overestimated and difficult to justify if one considers the chemical bondings in  $\text{Li}_2\text{VOSiO}_4$  structure. Therefore,

a purely 2D order should be observable only for  $T_c - T \lesssim 0.2$  K.

Although the nature of this phase transition remains to be clarified, one can argue that the insensitivity both of the Néel temperature and of the critical exponent of the sublattice magnetization to the magnetic field indicates that the phase transition is driven by the XY anisotropy.

In 3D magnets with two or more possible pitch vectors  $\mathbf{Q}$ , the ordering usually corresponds to a choice of pitch vector. The situation is often more complicated at lower temperature, and further transitions corresponding to other combinations of the pitch vectors or to the appearance of higher harmonics have been reported. Besides, the relevant parameter for the nature of the transition is the product  $N = n \times m$ , where  $n$  is the number of components of the order parameter (3 for Heisenberg) and  $m$  is the number of equivalent wave-vectors<sup>27</sup>. As a consequence, the resulting transition can have a large critical exponent  $\beta$ , typically around 0.4, or might in some cases be discontinuous.

The results reported in the present paper suggest that the transition is split into two transitions: First a structural transition, as revealed by Si NMR, then an ordering transition, as seen at the Li site. A natural question arises as to whether the Ising degree of freedom corresponding to the two possible collinear states is associated with the structural distortion or with the magnetic ordering. We believe that the first possibility is the most likely both on experimental and theoretical grounds. Experimentally, the small value of the exponent  $\beta$  is typical of layered magnets with XY symmetry. If the parameter  $N$  was increased by a factor 2 with respect to the number of components of the order parameter due to the Ising degree of freedom, one would not expect to observe such a small exponent. Besides, the choice of a pitch vector for the collinear phase renders the two directions inequivalent, and this is likely to be coupled to the lattice and to be associated with a structural distortion.

One has to notice that the structural distortion occurring just above  $T_c$  may have modified the spin hamiltonian. Therefore, a discussion of the properties of the ordered phase on the basis of the parameters extracted above  $T_c$  could be misleading. Nevertheless, one has to notice that, to be consistent with a collinear order,  $J_2/J_1$  must be larger than  $\simeq 0.65$  also

below  $T_c$ .

Information on the coupling constants below  $T_c$  can be derived from the  $T$  dependence of  ${}^7\text{Li}$  nuclear spin-lattice relaxation. Below  $T_c$   ${}^7\text{Li}$   $1/T_1$  is mainly driven by two-magnon Raman processes<sup>28</sup>, leading to a  $T^3$   $T$  dependence for  $T \gg \Delta$ , the gap in the spin-wave spectrum, and to  $1/T_1 \propto T^2 \exp(-\Delta/T)$  for  $T \ll \Delta$ . The low  $T$  dependence of  ${}^7\text{Li}$   $1/T_1$  turns out to be activated and, by fitting the data for  $T \leq 2.2$  K with the latter expression, one finds  $\Delta = 6 \pm 1$  K<sup>29</sup>. This value of the spin-wave gap is quite large if compared to the value of  $\Theta = J_1 + J_2$ , estimated from susceptibility measurements above  $T_c$ , and would imply an axial anisotropy  $D \simeq \Theta = 8.2 \pm 1$  K ( $D \sim \Delta^2/(J_1 + J_2)$ ), which is quite large for  $\text{V}^{4+}$ . In fact, the values of the  $g$  factor estimated from ESR measurements are very close to 2 and yield a value of  $D < 1$  K<sup>21</sup>. Moreover, if  $D \simeq \Theta$   $\text{Li}_2\text{VOSiO}_4$  should behave as an Ising system, not as an XY or Heisenberg one, in sharp contrast to the experimental findings. Thus, one is tempted to argue that the low  $T$  collinear phase is characterized by coupling constants slightly larger than the ones determined above  $T_c$ , so that  $D \ll J_1 + J_2$  and its absolute value is smaller.

Finally, one has to expect that frustration also causes a reduction of the staggered magnetization due to the enhancement of quantum fluctuations. The  $T \rightarrow 0$  average magnetic moment of  $\text{V}^{4+}$  ions can be obtained from  ${}^7\text{Li}$  NMR spectra below  $T_c$ . By extrapolating to  $T \rightarrow 0$  the splitting of  ${}^7\text{Li}$  NMR satellites and taking into account the hyperfine couplings given by Eq. 6, one can estimate a  $\text{V}^{4+}$  magnetic moment  $\mu(T \rightarrow 0) \simeq 0.24\mu_B$ . This value is reduced not only with respect to the value  $0.65\mu_B$  expected for a non-frustrated 2DQHAF, but also with respect to the value derived numerically by Schulz et al.<sup>20</sup> for  $J_2/J_1 \simeq 1$ , suggesting that probably below  $T_c$   $J_2/J_1 \lesssim 1$ .

#### IV. CONCLUSION

In conclusion, it has been shown that  $\text{Li}_2\text{VOSiO}_4$  is a prototype of a frustrated 2DQHAF on a square lattice with  $J_2/J_1 \simeq 1.1$  and  $J_2 + J_1 = 8.2 \pm 1$  K. Its ground state is a collinear

phase, as expected for  $J_2/J_1 \gtrsim 0.65$ . The phase diagram as a function of the magnetic field intensity is characterized by a constant  $T_c(H)$ , for  $0 \leq H \leq 9$  Tesla. This observation, together with the fact that the critical exponent of the magnetization  $\beta \simeq 0.235$ , suggest that the transition to the collinear phase is driven by the XY anisotropy. The structural distortion occurring just above  $T_c$ , is expected to lift the degeneracy between the two collinear ground states and to modify the superexchange couplings. In order to gain further insights on the nature of the phase transition and on the effective coupling constants below  $T_c$  further measurements with other techniques (e.g. inelastic neutron scattering) are required.

## V. ACKNOWLEDGMENTS

A. Lascialfari and J. S. Lord are acknowledged for their help during the SQUID and  $\mu$ SR measurements, respectively. M. C. Mozzati is thanked for the crystal field calculations. Fruitful discussions with L. Capriotti, A. Rigamonti, S. Sorella and R. Vaia are gratefully acknowledged.



## REFERENCES

- <sup>1</sup> see for example E. Dagotto and T. M. Rice, Science 271, 619 (1995) and E. Dagotto, Rep. Prog. Phys. 62, 1525 (1999) and references therein
- <sup>2</sup> D. Pines, Z. Phys. B 103, 129 (1997)
- <sup>3</sup> P. Chandra and B. Doucot, Phys. Rev. B 38, 9335 (1988)
- <sup>4</sup> H. J. Schulz and T. A. L. Ziman, Europhys. Lett. 18, 355 (1992); H. J. Schulz, T. A. L. Ziman and D. Poilblanc, J. Phys. I (France) 6, 675 (1996)
- <sup>5</sup> S. Sorella, Phys. Rev. Lett. 80, 4558 (1998); L. Capriotti and S. Sorella, Phys. Rev. Lett. 84, 3173 (2000)
- <sup>6</sup> P. Chandra, P. Coleman and A. I. Larkin, Phys. Rev. Lett. 64, 88 (1990)
- <sup>7</sup> Y. J. Kim et al., Phys. Rev. Lett. 83, 852 (1999); Y. J. Kim et al., cond-mat/0009314; R. Coldea et al., cond-mat/0007172
- <sup>8</sup> R. Melzi et al., Phys. Rev. Lett. 85, 1318 (2000)
- <sup>9</sup> P. Millet and C. Satto, Mat. Res. Bull. 33, 1339 (1998)
- <sup>10</sup> The error bar of  $\pm 1$  K accounts for the systematic dependence of  $\Theta$ , derived from Eq. 2, on the temperature range.
- <sup>11</sup> Crystal field calculations, performed taking into account the five oxygens forming  $V^{4+}$  pyramidal environment yield the following energy splitting of the  $3d$  orbitals (in eV)  $E_{d_{xy}} = -0.272$ ,  $E_{d_{xz}} = E_{d_{yz}} = -0.093$ ,  $E_{d_{x^2-y^2}} = 0.117$  and  $E_{d_{3z^2-r^2}} = 0.342$ .
- <sup>12</sup> A. Schenck in *Muon Spin Rotation: Principles and Applications in Solid State Physics* (Hilger, Bristol 1986)
- <sup>13</sup> On the basis of a point charge approximation one derives an electric field gradient tensor at  $^7\text{Li}$  nuclei with its main axis tilted by  $\simeq 40$  degrees from the  $c$  axis and a quadrupolar

frequency of  $\simeq 140$  kHz, yielding a shift of  $\pm 1/2 \rightarrow \pm 3/2$  resonance frequency from the central resonance of  $\simeq 60$  kHz, close to the one experimentally observed.

<sup>14</sup> M. Troyer, private communication

<sup>15</sup> R. R. P. Singh and R. Narayanan, Phys. Rev. Lett. 65, 1072 (1990)

<sup>16</sup> S. Bacci, E. Gagliano and E. Dagotto, Phys. Rev. B 44, 285 (1991)

<sup>17</sup> see H. Benner and J. P. Boucher in *Magnetic Properties of Layered Transition Metal Compounds*, Ed. L. J. de Jongh (Dodrecht, Kluwer), p. 323 (1990)

<sup>18</sup> A. Rigamonti, F. Borsa and P. Carretta, Rep. Prog. Phys. 61, 1367 (1998); A. V. Chubukov, S. Sachdev and J. Ye, Phys. Rev. B 49, 11919 (1994)

<sup>19</sup> P. Carretta et al., Phys. Rev. Lett. 84, 366 (2000)

<sup>20</sup> H. J. Schulz, T. A. L. Ziman and D. Poilblanc, J. Phys. I France 6, 675 (1996)

<sup>21</sup> V. Pashchenko, Y. Ksari and A. Stepanov, unpublished.

<sup>22</sup> see H. J. M. de Groot and L. J. de Jongh in *Magnetic Properties of Layered Transition Metal Compounds*, Ed. L. J. de Jongh (Dodrecht, Kluwer), p. 379 (1990); see also O. A. Petrenko, A. Honecker and M. E. Zhitomirsky, cond-mat/0003343

<sup>23</sup> S. T. Bramwell and P. C. W. Holdsworth, Phys. Rev. B 49, 8811 (1994); S. T. Bramwell and P. C. W. Holdsworth, J. Phys.: Condens. Matter 5, L53 (1993)

<sup>24</sup> B. J. Suh et al., Phys. Rev. Lett. 75, 2212 (1995)

<sup>25</sup> H. -Q. Ding, Phys. Rev. Lett. 68, 1927 (1992)

<sup>26</sup> D. C. Johnston in *Handbook of Magnetic Materials* vol 10, Ed. K. H. J. Buschow (Amsterdam, North Holland) ch 1, p. 1

<sup>27</sup> See e.g. the discussion in “Rare Earth Magnetism”, by J. Jensen and A. R. Mackintosh, Oxford Science Publications (1991), and references therein.

<sup>28</sup> D. Beeman and P. Pincus, Phys. Rev. 166, 359 (1968)

<sup>29</sup> This value of  $\Delta$  is reduced with respect to the value ( $\Delta \simeq 18$  K) previously reported in Ref. 8. The reason is that in Ref. 8  $1/T_1$  has been fitted with a simple Arrhenius law, without the  $T^2$  prefactor, and over a  $T$  range limited to higher temperatures.

## FIGURES

FIG. 1. a) Schematic phase diagram of a frustrated 2DQHAF on a square lattice as a function of the ratio  $J_2/J_1$  of the superexchange couplings. b) Structure of  $\text{Li}_2\text{VOSiO}_4$  projected along [001].  $\text{SiO}_4$  tetrahedra are in gray,  $\text{VO}_5$  pyramids are in black while the gray circles indicate  $\text{Li}^+$  position. For details see Ref. 9.

FIG. 2. a) Temperature dependence of  $\text{Li}_2\text{VOSiO}_4$  molar specific heat below 70 K. The solid lines shows the phonon contribution to  $C(T)$ , according to Eq. 1 in the text, with  $\Theta_D = 280$  K. b) Magnetic contribution to the specific heat, obtained after subtracting the phonon term corresponding to the solid line in a)

FIG. 3. Temperature dependence of the susceptibility  $\chi = M/H$ , for  $H = 3$  kGauss, in  $\text{Li}_2\text{VOSiO}_4$  powders. The dashed line shows the best fit according to Eq. 2, for  $15 \leq T \leq 300$  K. In the upper inset the derivative  $d\chi/dT$  is reported, evidencing a phase transition around 2.8 K. In the lower inset magnetization measurements in a  $\text{Li}_2\text{VOSiO}_4$  single crystal, both for  $H$  parallel and perpendicular to the  $c$  axis are reported. The intensity of  $M$  for  $\vec{H} \perp c$  have been rescaled for the sake of comparison.

FIG. 4. Magnetic field versus  $T$  phase diagram for  $\text{Li}_2\text{VOSiO}_4$ . The circles indicate the field dependence of  $T_c$  derived from the kink in the susceptibility and/or from the peak in  $d\chi/dT$  (see Fig. 3), while the squares the corresponding values of  $T_c$  determined from  $^7\text{Li}$  NMR spectra (see Fig. 10).

FIG. 5. Time evolution of  $\mu^+$  polarization in  $\text{Li}_2\text{VOSiO}_4$  powders for  $T$  close to  $T_c$ . The solid regular line shows the best fit according to Eq. 3 in the text. The T stability was within  $\pm 5 \times 10^{-3}$  K.

FIG. 6. Temperature dependence of the local field at the muon in  $\text{Li}_2\text{VOSiO}_4$  powders, derived from ZF $\mu$ SR measurements. The dashed line indicates the critical behaviour for a critical exponent of the magnetization  $\beta = 0.235 \pm 0.009$  (see text).

FIG. 7. Temperature dependence of the muon longitudinal relaxation rate in  $\text{Li}_2\text{VOSiO}_4$  powders. The solid line indicates the  $T$  dependence of  $\lambda$  according to Eq. 10, with a spin stiffness  $\rho_s = 7.4/2\pi$  K.

FIG. 8. Plot of  $^7\text{Li}$  NMR paramagnetic shift versus the macroscopic susceptibility in  $\text{Li}_2\text{VOSiO}_4$ , for  $H \parallel c$ . The solid line shows the best fit yielding a total hyperfine coupling of 2.6 kGauss and a chemical shift  $\delta = -70 \pm 30$  ppm, for  $\vec{H} \parallel c$ .

FIG. 9.  $^7\text{Li}$  NMR spectra for  $H = 1.8$  Tesla along the  $c$  axis in a  $\text{Li}_2\text{VOSiO}_4$  single crystal, in the proximity of  $T_c$ .

FIG. 10. Temperature dependence of the splitting of  $^7\text{Li}$  NMR satellites, for  $H = 1.8$  Tesla along the  $c$  axis. The solid line shows the critical behaviour for an exponent  $\beta = 0.24$ .

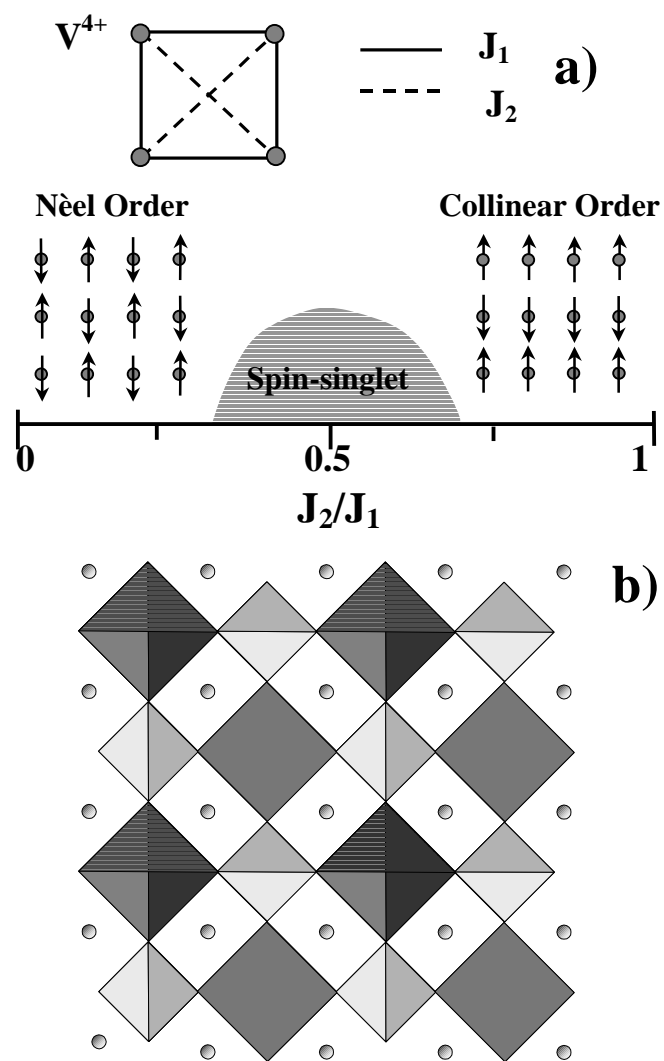
FIG. 11.  $^{29}\text{Si}$  NMR powder spectrum in  $\text{Li}_2\text{VOSiO}_4$  for  $H = 1.8$  Tesla in the proximity of  $T_c$ . The dotted lines mark the position of the peak at high and at low  $T$ .

FIG. 12.  $^7\text{Li}$  nuclear spin-lattice relaxation rate  $1/T_1$  for  $\vec{H} \parallel c$  in  $\text{Li}_2\text{VOSiO}_4$ , for  $H = 1.8$  Tesla (open squares) and 9 Tesla (closed circles). The dotted line gives the best fit according to the expression for 2-magnon relaxation processes (see text), yielding  $\Delta = 6 \pm 1$  K. In the inset the corresponding  $T$  dependence in the range 1.6 to 100 K is reported.

FIG. 13.  $^{29}\text{Si}$  NMR  $1/T_1$  in  $\text{Li}_2\text{VOSiO}_4$  for  $H = 1.8$  Tesla, for  $T \leq 4.2$  K.

FIG. 14. a) Amplitude of the maximum in the molar specific heat for a frustrated 2DQHAF versus  $J_2/J_1$ . The open squares represent the data derived from Ref. 15, while the closed circles derived from Ref. 16. The gray region around  $C^m(T_m^C)/R = 0.436$  represents the experimental value for this quantity, inclusive of the error bar. b)  $T_m^C/J_1$  (see text) versus  $J_2/J_1$  derived from Ref. 15. The solid lines show the behaviour according to Eq. 7, for values of  $\Theta$  corresponding to the lower and upper limits of the Curie-Weiss temperature estimated from susceptibility measurements.

Fig.1 (R. Melzi et al.)



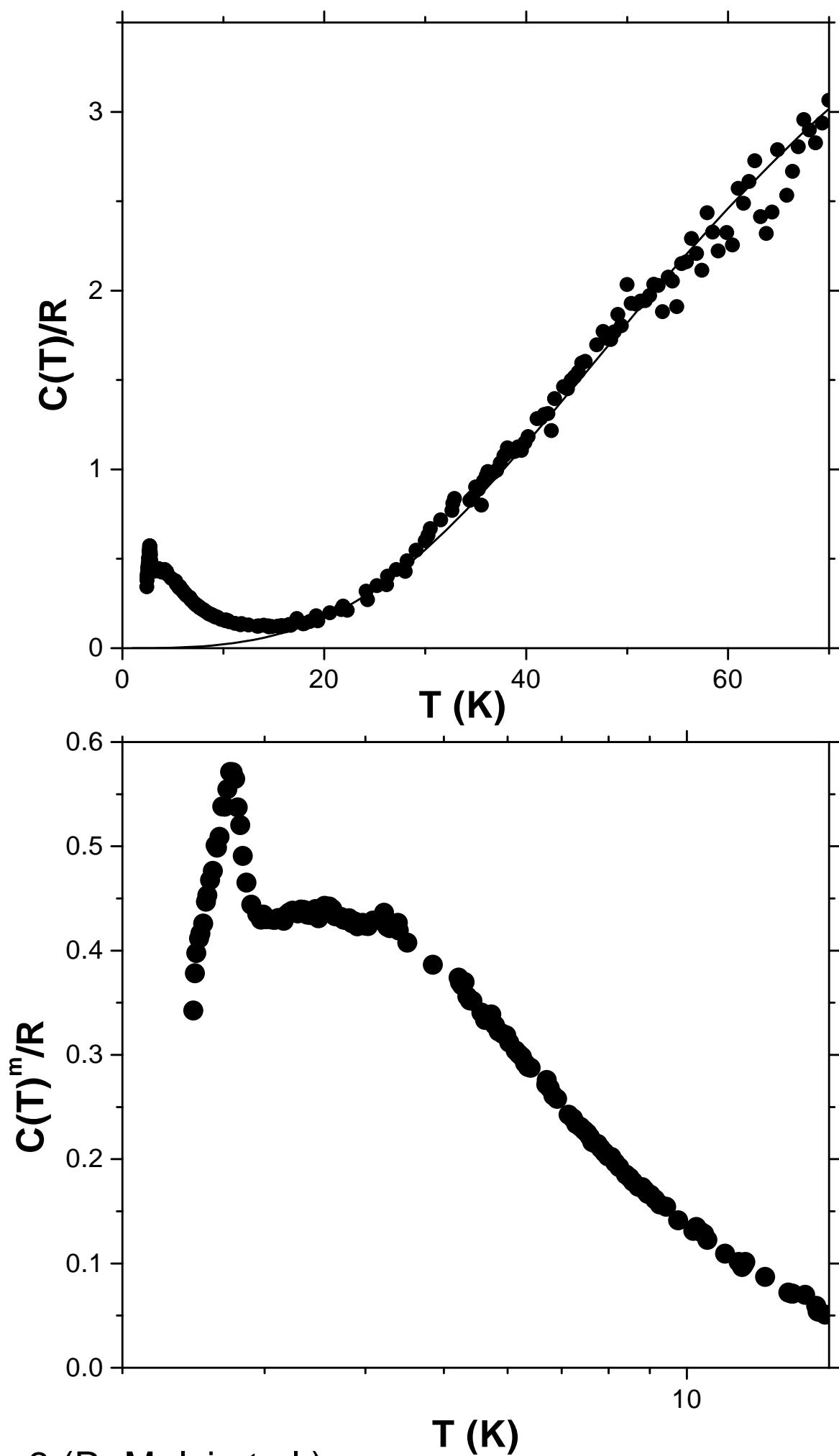


Fig.2 (R. Melzi et al.)

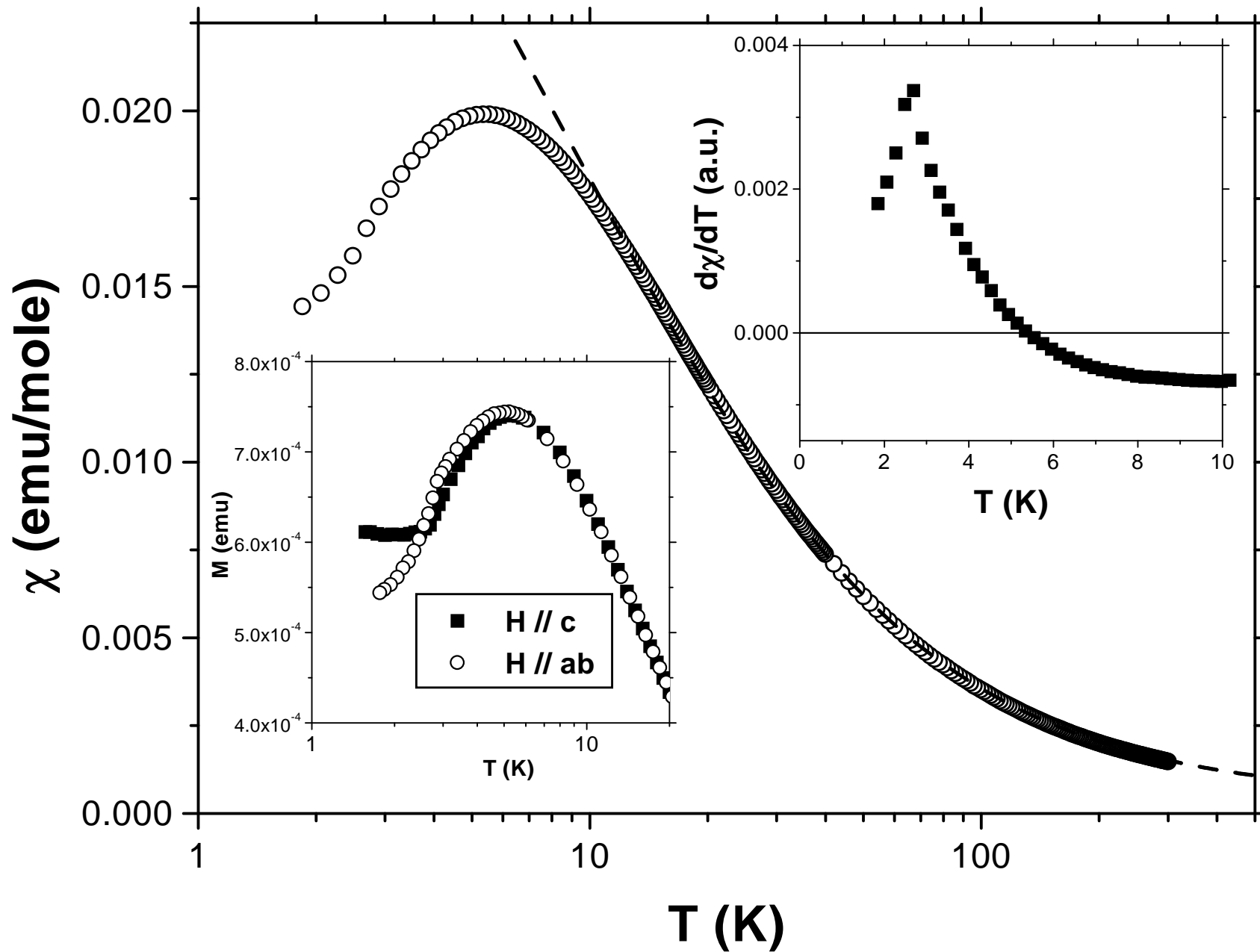


Fig.3 (R. Melzi et al.)



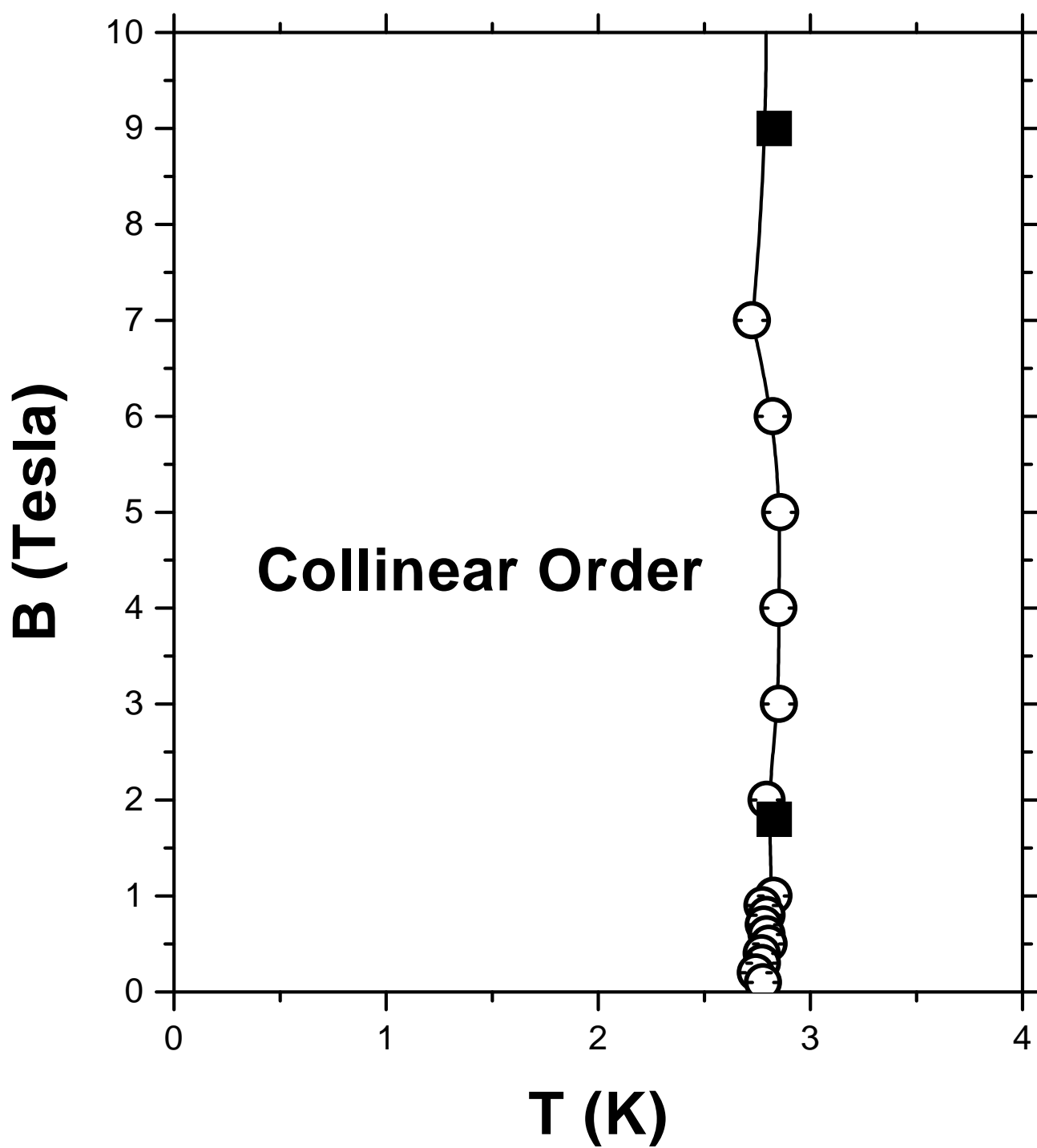
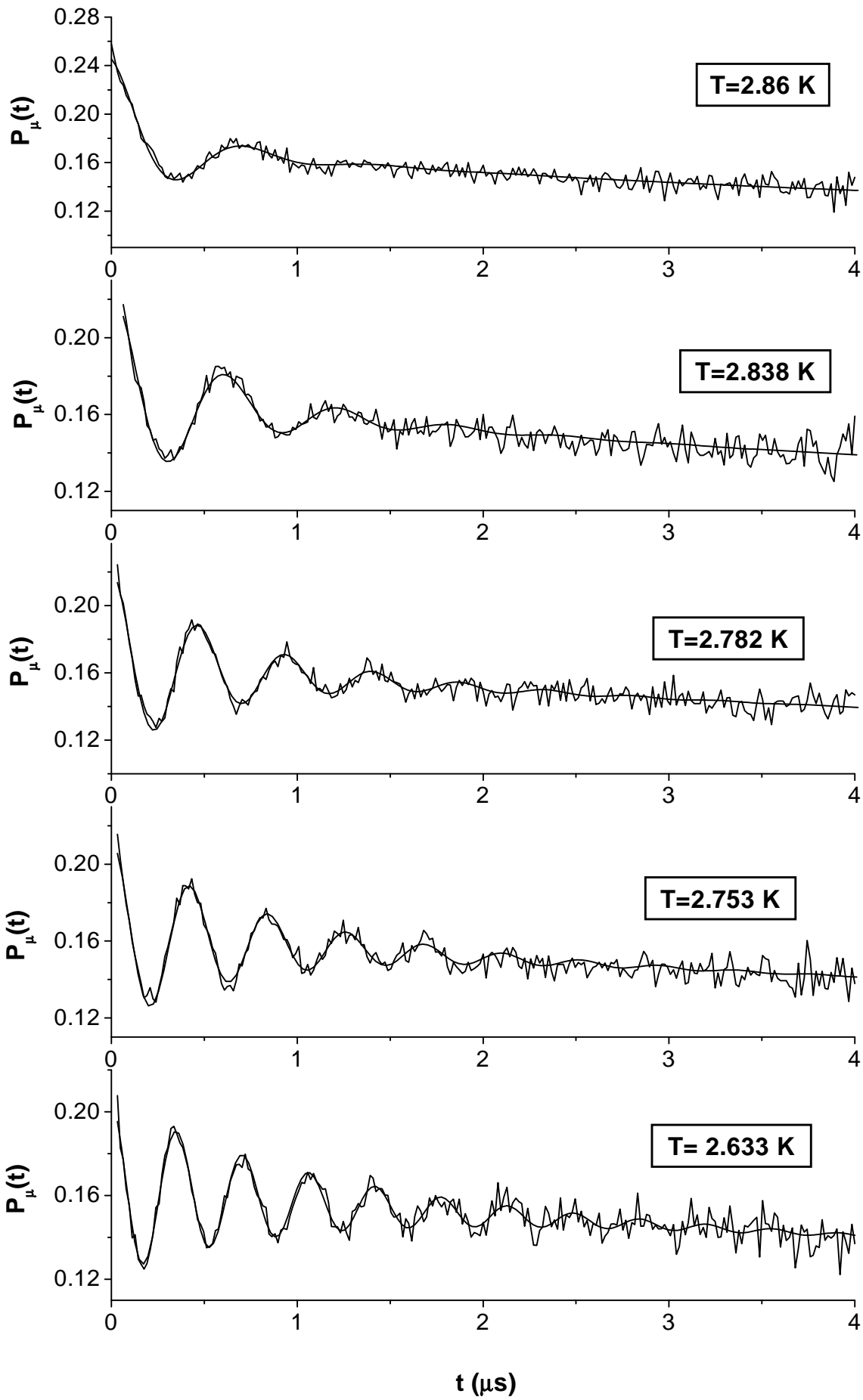


Fig.4 (R. Melzi et al.)

Fig.5 (R. Melzi et al.)



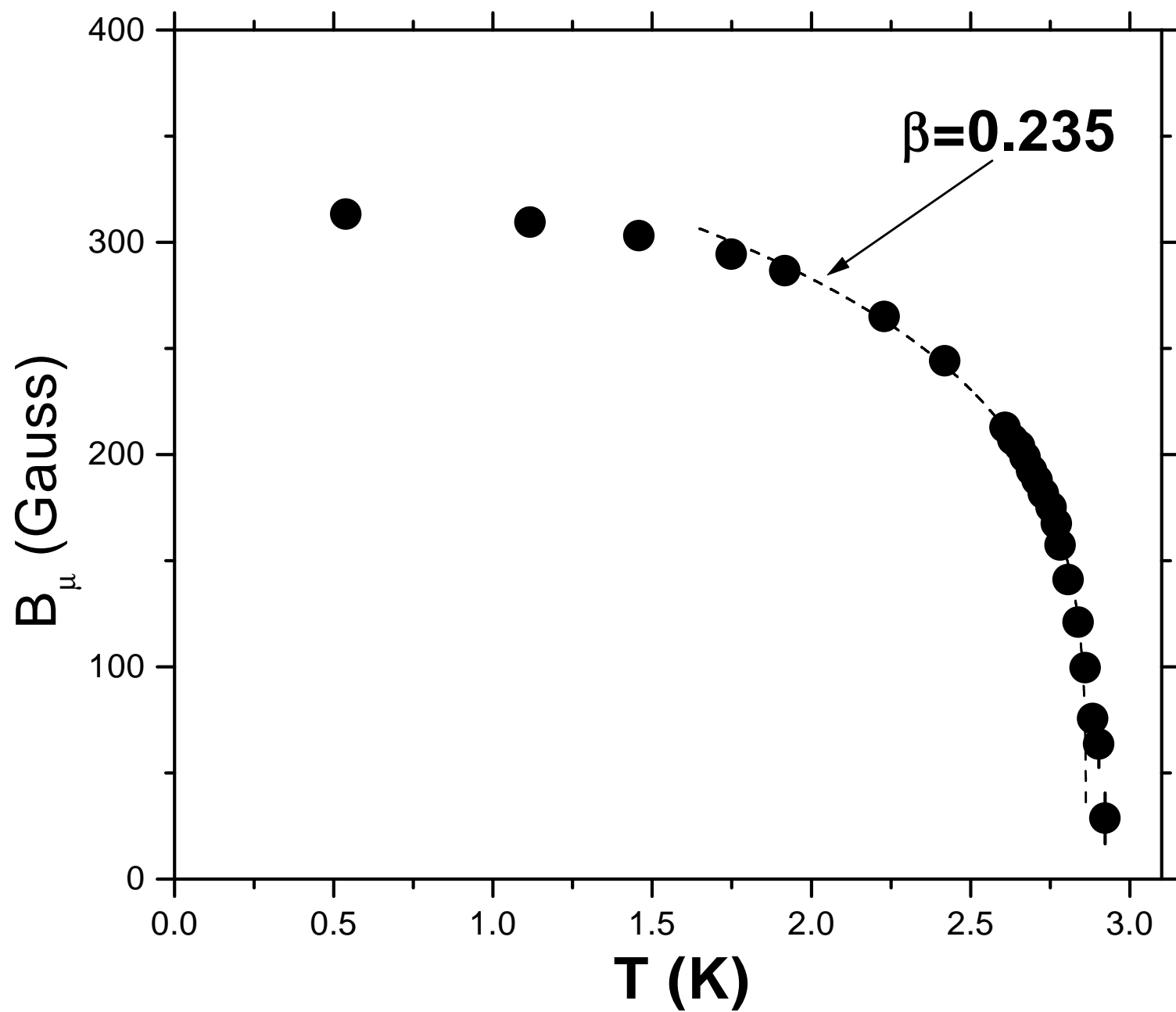


Fig.6 (R. Melzi et al.)

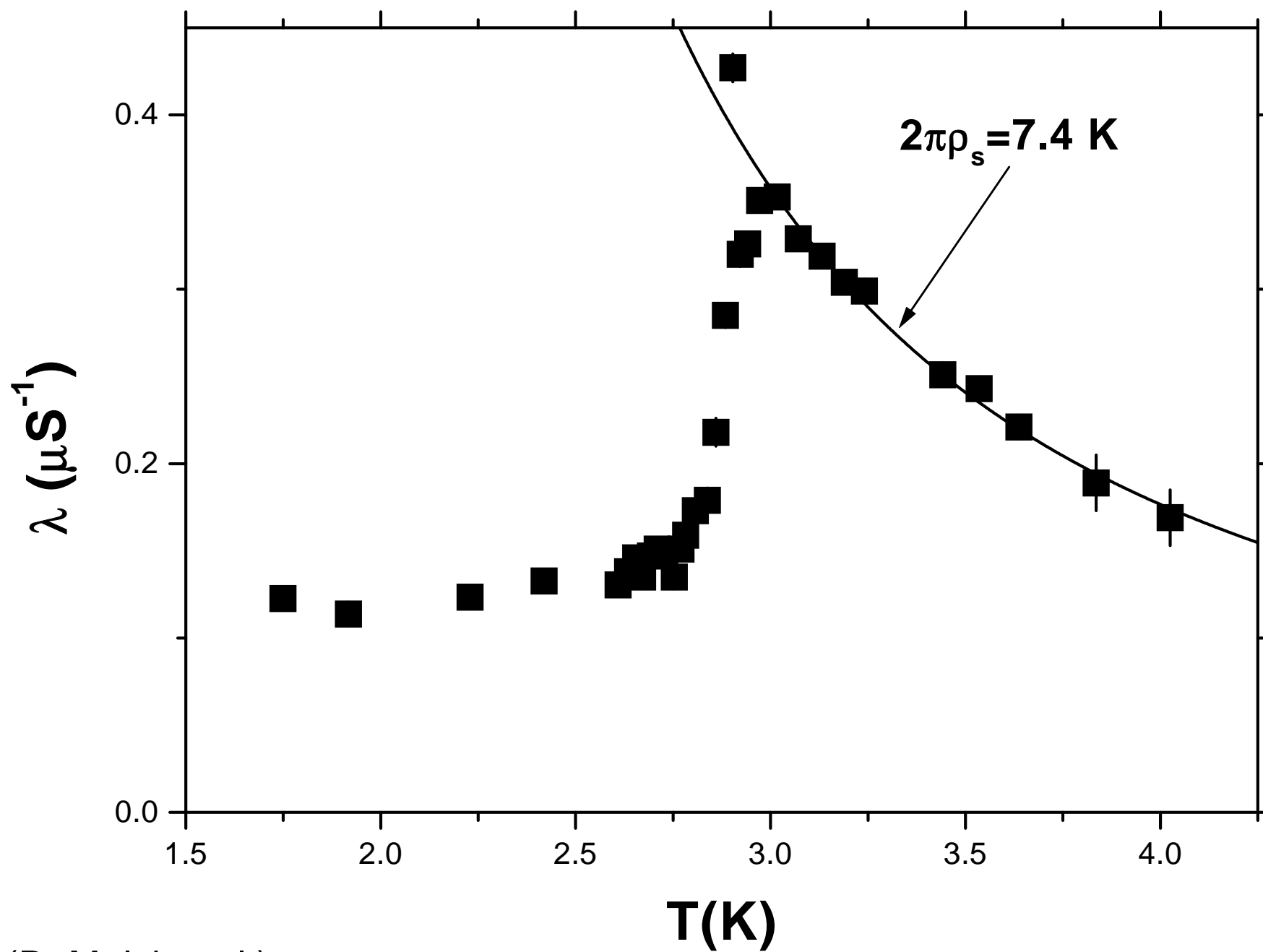


Fig.7 (R. Melzi et al.)

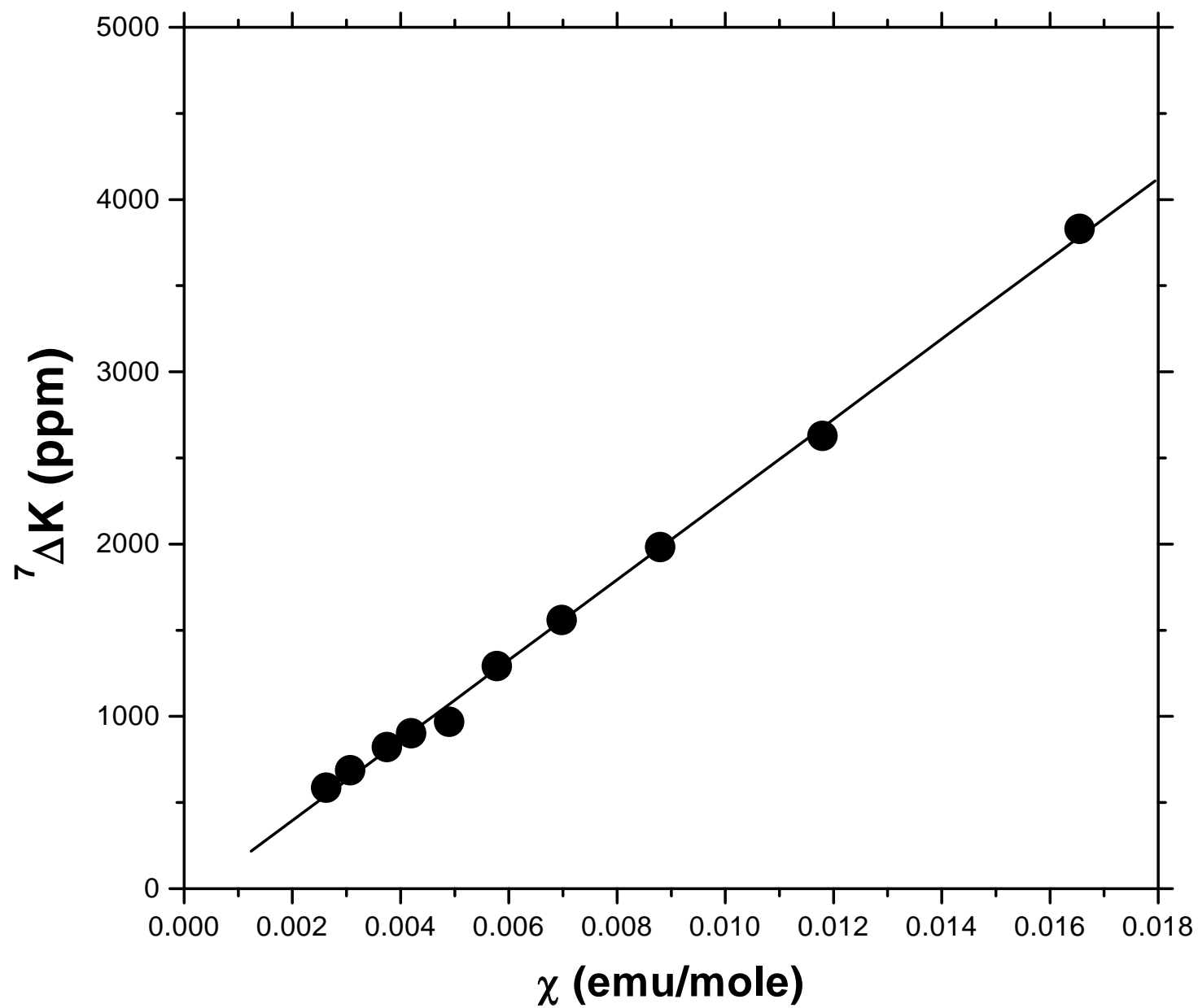


Fig.8 (R. Melzi et al.)

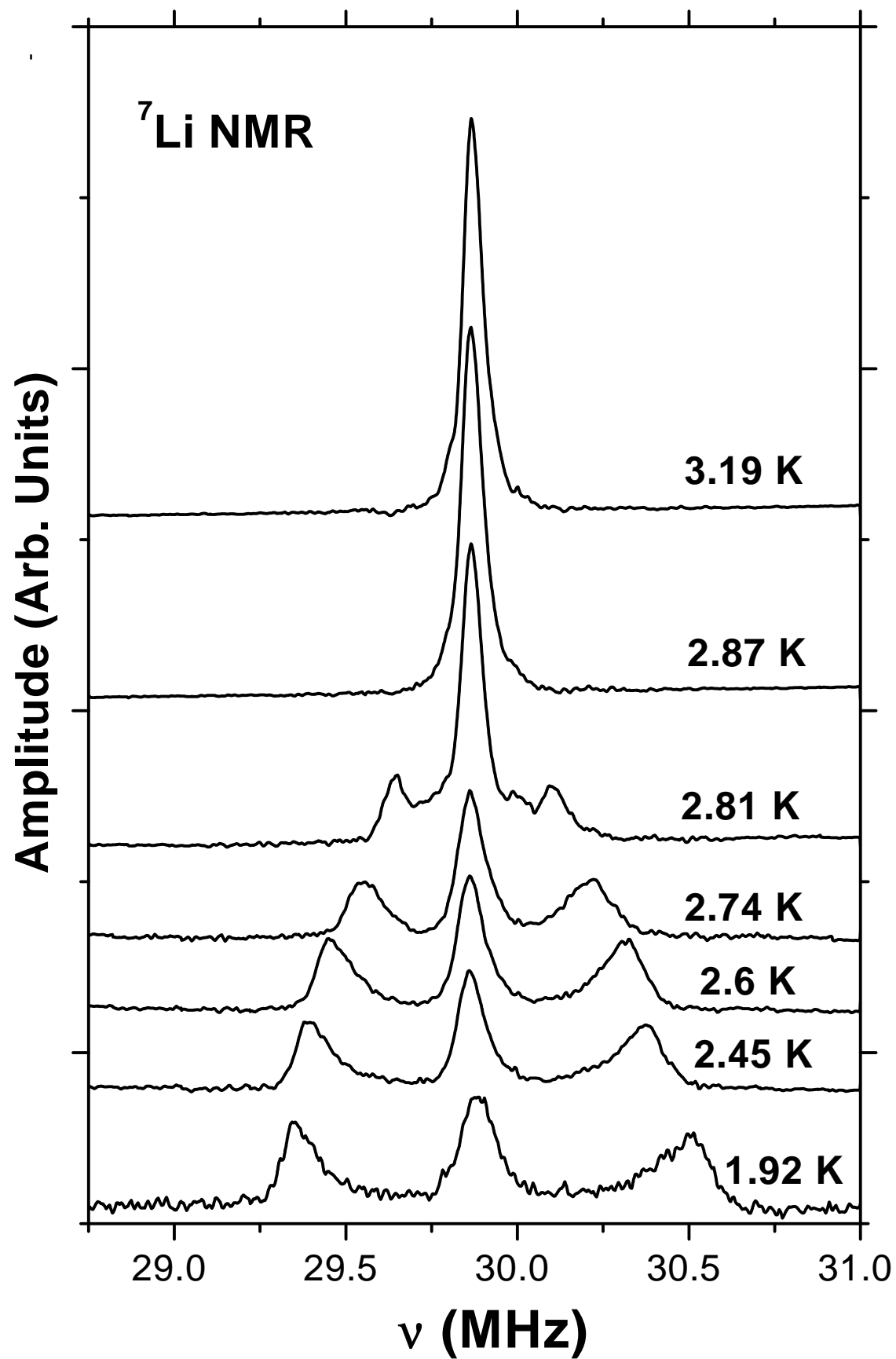


Fig. 9 (R. Melzi et al.)

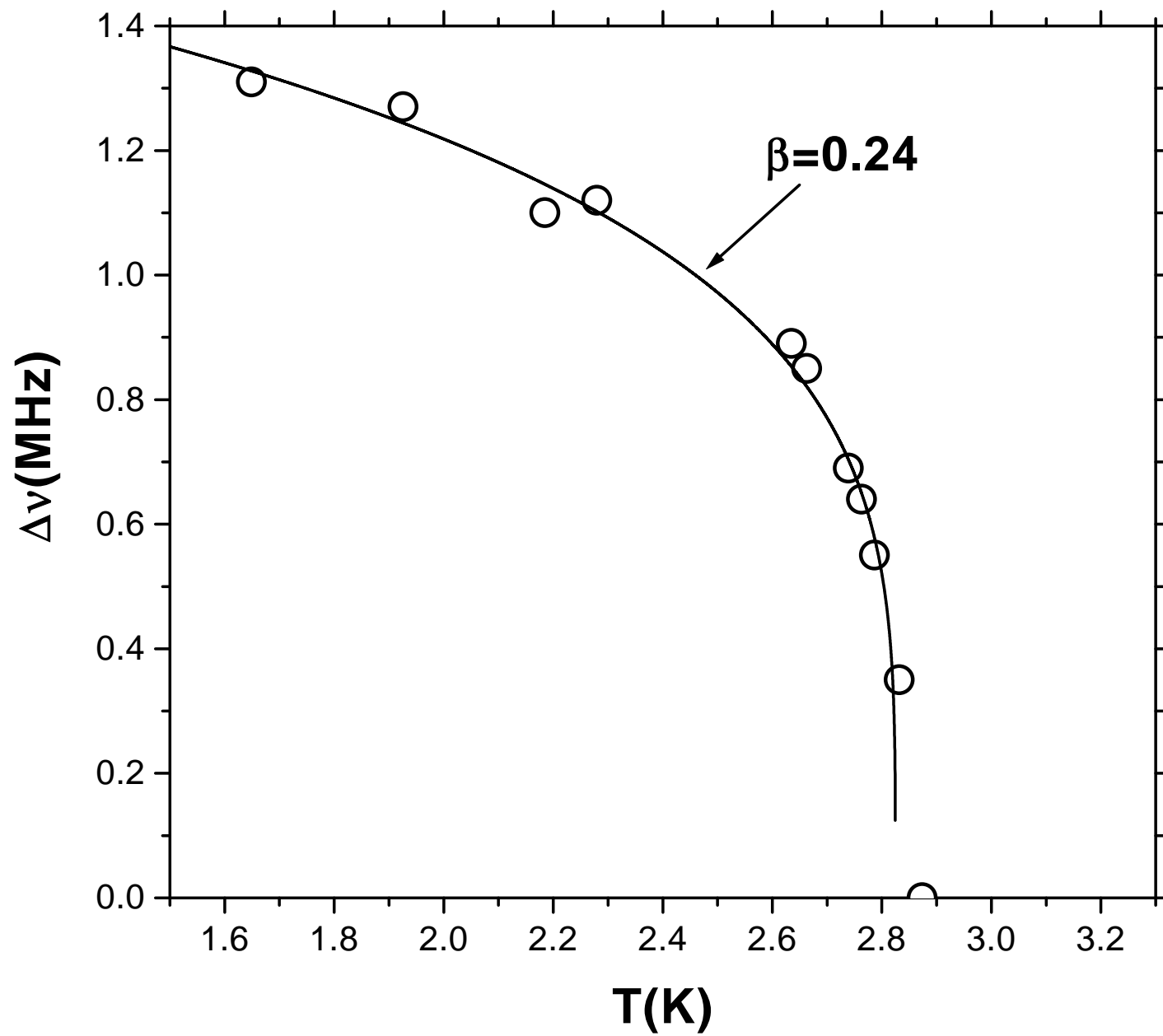


Fig. 10 (R. Melzi et al.)

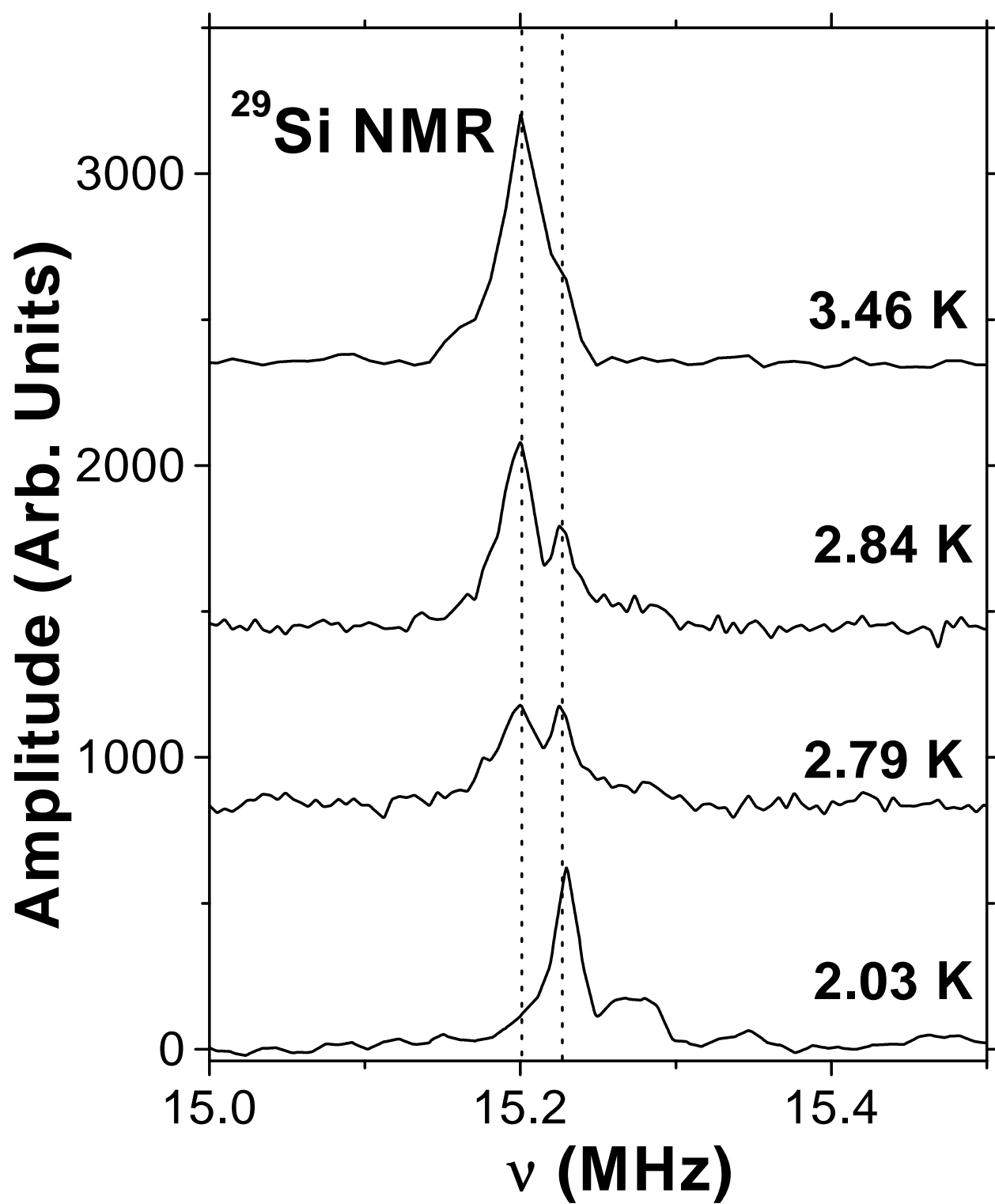


Fig. 11 (R. Melzi et al.)



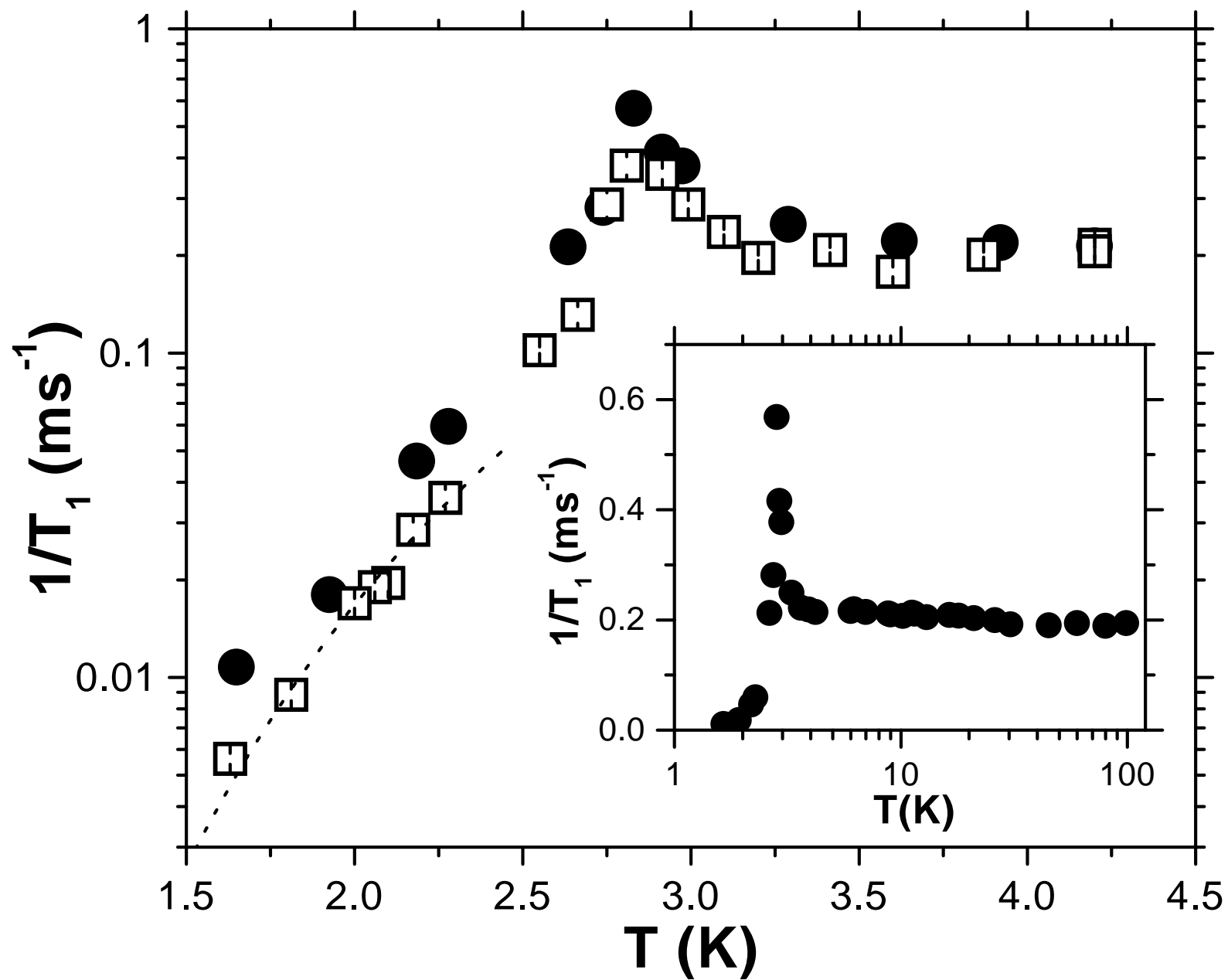


Fig. 12 (R. Melzi et al.)

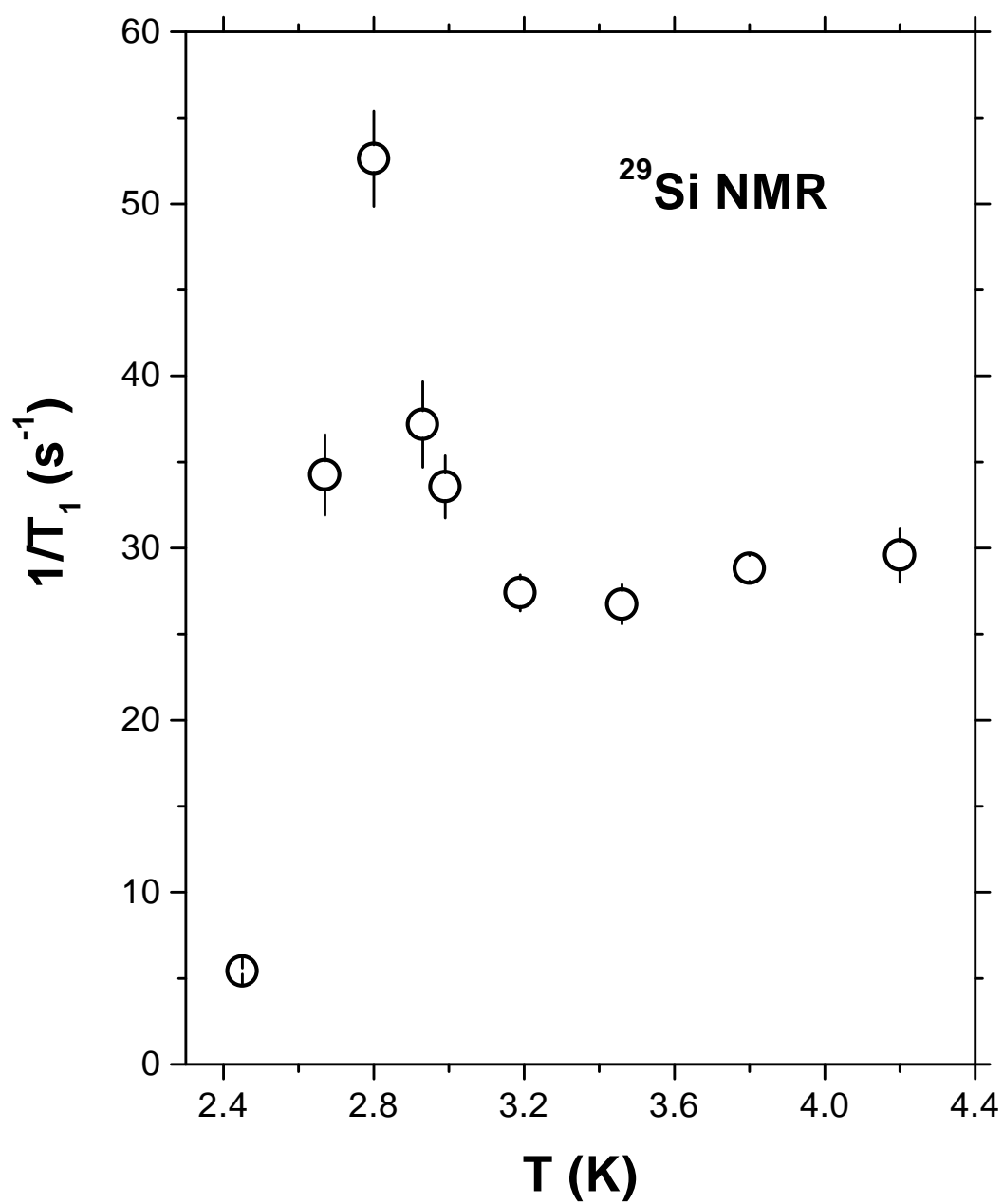


Fig. 13 (R. Melzi et al.)

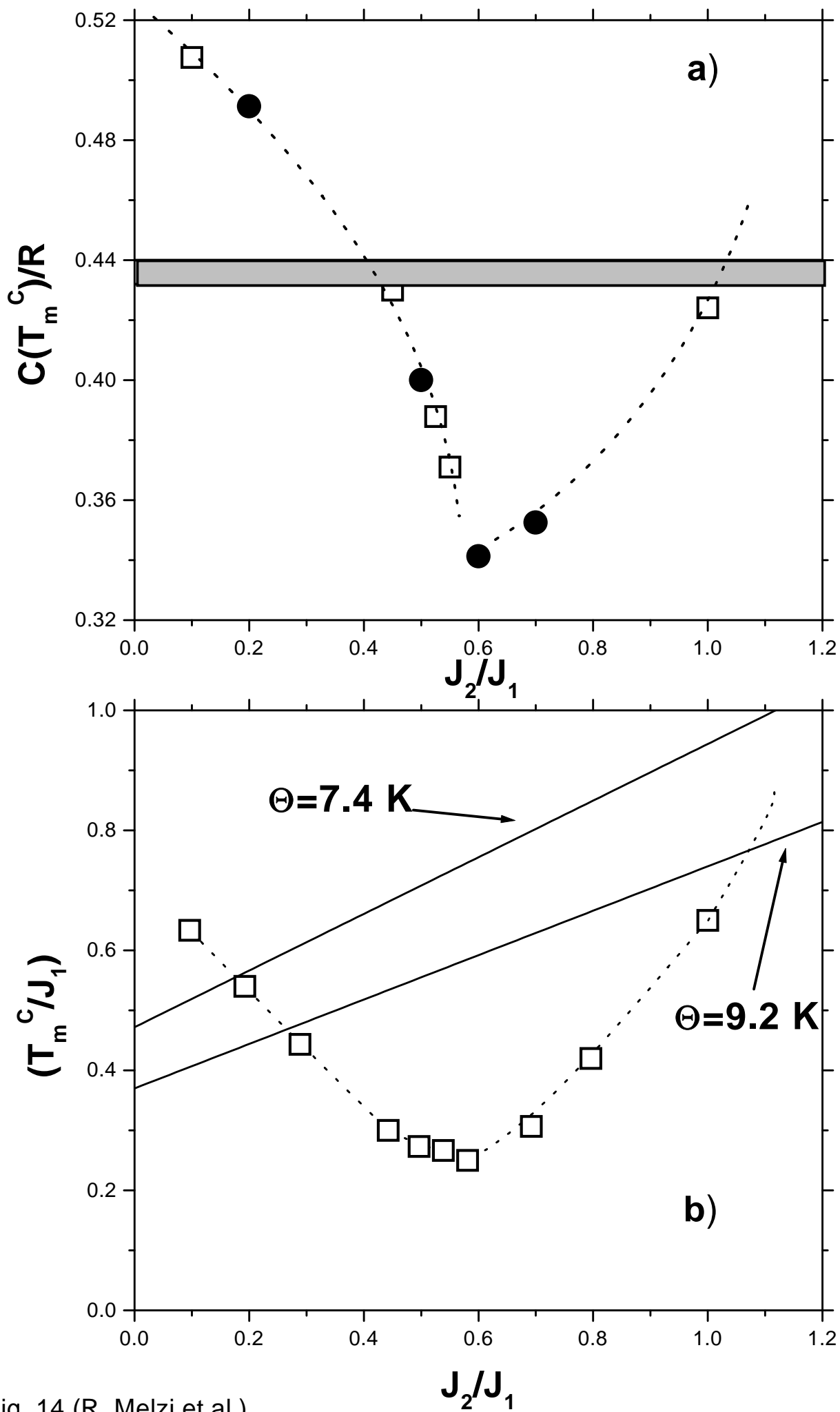


Fig. 14 (R. Melzi et al.)